

Particle based method for shallow landslides: modeling sliding surface lubrication by rainfall

Emanuele Massaro¹, Gianluca Martelloni^{1,2}, and Franco Bagnoli¹

¹ Department of Energy "Sergio Stecco", University of Florence, Italy
(E-mail: emanuele.massaro@unifi.it, franco.bagnoli@unifi.it)

² Earth Sciences Department, University of Florence, Italy
(E-mail: gianluca.martelloni@unifi.it)

Abstract. Landslides are a recurrent phenomenon in many regions of Italy: in particular, the rain-induced shallow landslides represent a large percentage of this type of phenomenon, responsible of human life loss, destruction of assets and infrastructure and other major economical losses. In this paper a theoretical computational mesoscopic model based on interacting particles has been developed to describe the features of a granular material along a slope. We use a Lagrangian method similar to molecular dynamic (MD) for the computation of the movement of particles after and during a rainfall. In order to model frictional forces, the MD method is complemented by additional conditions: the forces acting on a particle can cause its displacement if they exceed the static friction between them and the slope surface, based on the failure criterion of Mohr-Coulomb, and if the resulting speed is larger than a given threshold. Preliminary results are very satisfactory; in our simulations emerging phenomena such as fractures and detachments can be observed. In particular, the model reproduces well the energy and time distribution of avalanches, analogous to the observed Gutenberg-Richter and Omori distributions for earthquakes. These power laws are in general considered the signature of self-organizing phenomena. As in other models, this self organization is related to a large separation of time scales between rain events and landslide movements. The main advantage of these particle methods is given by the capability of following the trajectory of a single particle, possibly identifying its dynamical properties.

Keywords: Landslide, molecular dynamics, lagrangian modelling, particle based method, power law.

1 Introduction

Predicting natural hazards such as landslides, floods or earthquake is one of the challenging problems in earth science. With the rapid development of computers and advanced numerical methods, detailed mathematical models are increasingly being applied to the study of complex dynamical processes such as flow-like landslides and debris flows.



The term landslide has been defined in the literature as a movement of a mass of rock, debris or earth down a slope under the force of gravity [1,2]. Landslides occur in nature in very different ways. It is possible to classify them on the bases material involved and type of movement [3].

Landslides can be triggered by different factors but in most cases the trigger is an intense or long rain. Rainfall-induced landslides deserved a large interest in the international literature in the last decades with contributions from different fields, such as engineering geology, soil mechanics, hydrology and geomorphology [4]. In the literature, two approaches have been proposed to evaluate the dependence of landslides on rainfall measurements. The first approach relies on dynamical models while the second is based on the definition of empirical rainfall thresholds over which the triggering of one or more landslides can be possible [5]. At present, several methods has been developed to simulate the propagation of a landslide; most of the numerical methods are based on a continuum approach using an Eulerian point of view [6,7].

An alternative to these continuous approaches is given by discrete methods for which the material is represented as an ensemble of interacting but independent elements (also called units, particles or grains). The model explicitly reproduces the discrete nature of the discontinuities, which correspond to the boundaries of each element. The commonly adopted term for the numerical methods for discrete systems made of non deformable elements, is the discrete element method (DEM) and it is particularly suitable to model granular materials, debris flows and flow-like landslide [8]. The DEM is very closely related to molecular dynamics (MD), the former method is generally distinguished by its inclusion of rotational degrees-of-freedom as well as stateful contact and often complicated geometries. As usual, the more complex the individual element, the heavier is the computational load and the “smaller” is the resulting simulation, for a given computational power. On the other hand, the inclusion of a more detailed description of the units allows for more realistic simulations. However, the accuracy of the simulation has to be compared with the experimental data available. While for laboratory experiments it is possible to collect very accurate data, this is not possible for real-field landslides. And, finally, the proposed model is just an approximation of a much more complex dynamics. These arguments motivated us in exploring the consequences of reducing the complexity of the model as much as possible.

In this paper we present a simplified model, based on the MD approach, applied to the study of the starting and progression of shallow landslides, whose displacement is induced by rainfall. The main hypothesis of the model is that the static friction decreases as a result of the rain, which acts as a lubricant and increases the mass of the units. Although the model is still schematic, missing known constitutive relations, its emerging behavior is quite promising.

2 The model and simulation methodology

We limit the study to two-dimensional simulations (seen from above) along a slope, modeling shallow landslides. We consider N particles, initially arranged in a regular grid (Fig. 1), all of radius r and mass m .

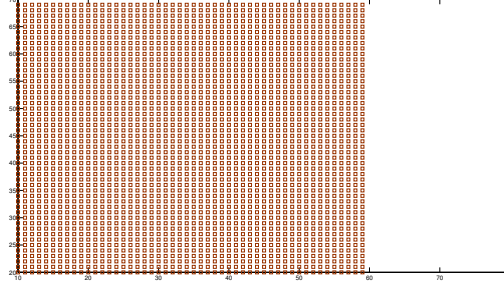


Fig. 1. Initial configuration of simulations. The 2500 particles are arranged on a regular grid of 50x50 cells of size 1×1 .

The idea is to simulate the dynamics of these particles during and after a rainfall. In the model the rain has two effects: the first causes an increase in the mass of particles, while the second involves a reduction in static friction between the particle and the surface below.

The equation of Mohr-Coulomb,

$$\tau_f = c' + \sigma' \tan(\phi'), \quad (1)$$

says that the shear stress τ_f on the sliding surface is given by an adhesive part c' plus a frictional part $\tan(\phi')$. In our model we want to find a trigger condition of the particle that is based on the law of Mohr-Coulomb (Eq. (1)). The coefficient of cohesion, c' in the Eq. (1), has been modeled by a random coefficient that depends on the position of the surface. On the other hand, the term $\sigma' \tan(\phi')$ in the Eq.(1), has been modeled by a theoretical force of static friction $F_i^{(s)}$ which is described later.

The static-dynamic transition is based on the following trigger conditions:

$$\begin{aligned} |\mathbf{F}_i^{(a)}| &< \mathbf{F}_i^{(s)} + c', \\ |\mathbf{v}_i| &< \mathbf{v}_i^{(threshold)} \rightarrow 0, \end{aligned} \quad (2)$$

then the motion of the single block will not be triggered until the active forces $\mathbf{F}_i^{(a)}$ (gravity forces + contact forces) do not exceed the static friction $\mathbf{F}_i^{(s)}$ plus the cohesion term c' and until the velocity $|\mathbf{v}_i|$ not overcomes the threshold velocity $\mathbf{v}_i^{(threshold)}$ (Eq. (2)). The irregularities of the surface are modeled by means of the friction coefficients, which depends stochastically on the position (quenched disorder).

In Eq. (2), the force $\mathbf{F}_i^{(a)}$ is given by the sum of two components: the gravity $\mathbf{F}_i^{(g)}$ and the interaction between the particles $\mathbf{F}_i^{(i)}$.

$$\mathbf{F}_i^{(a)} = \mathbf{F}_i^{(g)} + \mathbf{F}_i^{(i)}. \quad (3)$$

The gravity $\mathbf{F}_i^{(g)}$ is given by

$$\mathbf{F}_i^{(g)} = g \sin(\alpha)(m_i + w_i(t)), \quad (4)$$

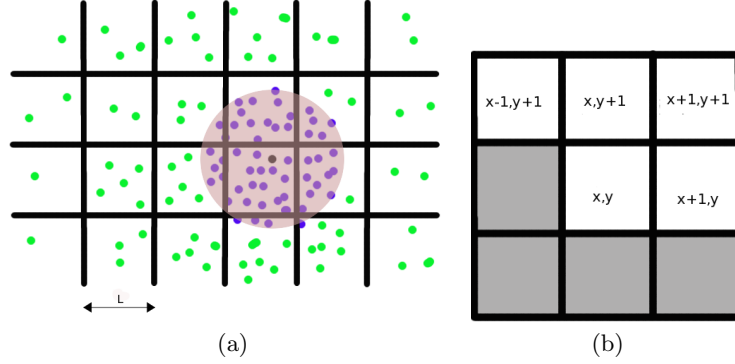


Fig. 2. (a) Particles in the computational domain: the maximum radius of iteration defined in the algorithm is equal to the side L of the cell. Considering the black particle in the center of the circumference, it can interact only with the neighboring blue particles. (b) Cells considered when calculating the forces: if a particle is in cell (x, y) , the interaction forces will be calculated considering only the particles located in cells $(x + 1, y)$, $(x + 1, y + 1)$, $(x + 1, y - 1)$ and $(x - 1, y)$. This method halves the number of interactions because it calculates 4 cells instead of 8.

where g is the acceleration of gravity, α the slope (supposed constant) of the surface, m_i the dry mass of block i and w_i the absorbed water cumulated in time. The quantity $w_i(t)$ is a stochastic variable (corresponding to rainfall events $\sigma^{(w)}(t)$),

$$w_i(t) = \int \sigma_i^{(w)}(t) dt. \quad (5)$$

The interaction force between two particles is defined through a potential that, in the absence of experimental data, we modeled after the Lennard-Jones one. The corresponding interaction force $\mathbf{F}_{ij}^{(i)}$ that acts on block i due to block j is given by

$$\mathbf{F}_{ij}^{(i)} = -\mathbf{F}_{ji}^{(i)} = -\nabla V(R_{ij}) = -\nabla \left(4\epsilon \cdot \left[\left(\frac{r}{R_{ij}} \right)^{-12} - \left(\frac{r}{R_{ij}} \right)^{-6} \right] \right), \quad (6)$$

where R_{ij} is the distance between the particles,

$$R_{ij} = \sqrt{(x_j - x_i)^2 + (y_j - y_i)^2}, \quad (7)$$

r is the radius of the particles and ϵ is a constant.

The computational strategy for calculating the interaction forces between the particles is similar to the Verlet neighbor list algorithm (art:verlet). In the code the computational domain is divided in square cells of side L (see Fig. 2 (a)), corresponding to the length at which the interaction force is truncated. The truncation has a very little effect on the dynamics, so we did not correct the potential by setting $V(L) = 0$, as usual in MD.

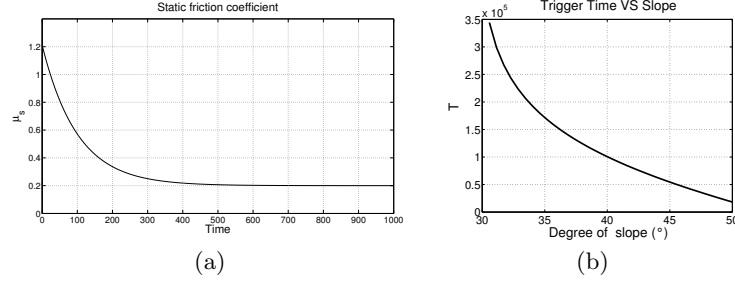


Fig. 3. (a) Static friction coefficient μ_s vs. time, with $\mu_s^{(0)} = 1.2$ and $\mu_s^{(\infty)} = 0.4$. (b) Triggering time vs. slope, Eq. 18 with $m = 0.01$, $c' = 0.1$, $\mu_s^{(0)} = 1.15$ and $\mu_s^{(\infty)} = 0.45$.

Thanks to the Newton's third law it is possible reduce the number interaction and consider the only particle that has not been considered in the previous step (see Fig. 2(b)).

The condition of motion for a given particle is governed by Eq. 2. The static friction $\mathbf{F}_i^{(s)}$ is given by

$$\mathbf{F}_i^{(s)} = \mu_s(m_i + w_i(t)) \cos(\alpha). \quad (8)$$

The Equation 8 is expressed by the friction's coefficient μ_s . We assumed that the rain has a lubricating effect between the particles and underlying surface; the friction coefficient has therefore been defined as,

$$\mu_s = \mu_s^{(\infty)} + (\mu_s^{(0)} - \mu_s^{(\infty)}) \exp(-w_0 t), \quad (9)$$

where $\mu_s^{(0)}$ and $\mu_s^{(\infty)}$ are, respectively, the initial (dry) friction coefficient at $t = 0$ (starting of rainfall) and the final (wet) for $t \rightarrow \infty$. The effect of rainfall is to lubricate the sliding surface of the landslide, at a constant speed w_0 in this example.

When the active forces exceed the static friction plus the quenched stochastic coefficient of cohesion c' , the particle start to move. In this case the force acting on the particle i is given by

$$\mathbf{F}_i = \mathbf{F}_i^{(a)} - \mathbf{F}_i^{(d)}, \quad (10)$$

where $\mathbf{F}_i^{(a)}$ are the active forces, and $\mathbf{F}_i^{(d)}$ is the force of dynamic friction,

$$\mathbf{F}_i^{(d)} = \mu_d(m_i + w_i(t)) \cos(\alpha). \quad (11)$$

Eq. (11) is of the same type as Eq. (8); the coefficient of dynamic friction μ_d is defined similarly to the static one (Eq. (9)). The friction coefficients (static and dynamic) varies from point to point of the computational domain this choice serves to model the sliding surface like a rough surface.

When a particle exceed the threshold condition (Eq. 2), it moves on the slope with an acceleration \mathbf{a} equal to

$$\mathbf{a} = \frac{\mathbf{F}_i}{(m_i + w_i(t))}. \quad (12)$$

In MD the most widely used algorithm for time integration is the Verlet algorithm. This algorithm allows a good numerical approximation and is very stable. It also does not require a large computational power because the forces are calculated once for each time step. The model was implemented using the second-order Verlet algorithm. We first compute the displacement of particles, and half of the velocity updates,

$$\begin{aligned} \mathbf{r}'_i &= \mathbf{r}_i + \mathbf{v}_i \Delta t + \frac{\mathbf{F}_i}{2m_i} \Delta t^2, \\ \mathbf{v}'_i &= \mathbf{v}_i + \frac{\mathbf{F}_i}{2m_i} \Delta t, \end{aligned} \quad (13)$$

then compute the forces \mathbf{F}'_i as function of the new positions \mathbf{r}'_i , and finally compute the second half of velocities,

$$\mathbf{v}''_i = \mathbf{v}'_i + \frac{\mathbf{F}'_i}{2m_i} \Delta t. \quad (14)$$

We have to define a landslide-triggering time, for instance the time of the first moving block. In case of constant mass, it is very simple to obtain the trigger time theoretically. We can write, in equilibrium conditions, for a given mass

$$\begin{aligned} |\mathbf{F}_i| &= \mathbf{F}_i^{(s)} + c' \\ \mathbf{F}_i &= \mathbf{F}_i^{(g)} + \mathbf{F}_i^{(i)} \end{aligned} \quad (15)$$

We assume that the first movement of the particle is only due to the effect of gravity, so that we can set the interaction forces equal to zero, and therefore the equilibrium condition is given by

$$|\mathbf{F}_i| = \mathbf{F}_i^{(g)} + c', \quad (16)$$

i.e.,

$$\hat{m}g \sin(\alpha) = \hat{m} \cdot g \cos(\alpha) \{ \mu_s^{(0)} \exp(w_0 \cdot t) + \mu_s^{(\infty)} [1 - \exp(-w_0 t)] \} + c', \quad (17)$$

where $\hat{m} = m + w(t)$, but Eq 17 is solvable analytically for $\hat{m} = m + \delta\omega$ ($\delta\omega$ is constant rain).

Therefore, using Eq 17 we can define the trigger time T in case of constant mass \hat{m} as:

$$T = -\frac{1}{w_0} \cdot \log \left(\frac{\tan(\alpha) - \frac{c'}{\hat{m}g \cos(\alpha)} - \mu_s^{(\infty)}}{\mu_s^{(0)} - \mu_s^{(\infty)}} \right). \quad (18)$$

Table 1. Parameter values used in simulations

Sim	m	r	cell	$\mu_s^{(0)}$	$\mu_s^{(\infty)}$	$\mu_d^{(0)}$	$\mu_d^{(\infty)}$	c'
1	0.0001	0.5	1x1	1.15	0.7	0.65	0.34	$0.01+\epsilon$
1b	0.0001	0.5	1x1	1.15	0.7	0.65	0.34	$0.01+\epsilon$
2	0.0001	0.5	1x1	1.15	0.7	0.65	0.34	$1+\epsilon$
3	0.0001	0.5	1x1	0.85	0.4	0.35	0.14	$0.01+\epsilon$

3 Results

In order to simulate a landslide along an inclined plane, we use the theoretical model as described above with different parameters.

In the Table 1 we illustrate the parameters used in different simulations, where Sim is the number of simulation, m and r are respectively the mass and the radius of the particles, $\mu_s^{(0)}$, $\mu_s^{(\infty)}$, $\mu_d^{(0)}$, $\mu_d^{(\infty)}$ are the coefficients of static and dynamic friction and c' is the coefficient of cohesion. In the our simulations the time dt of simulation is set to 0.01: then the effective time t is different from the simulation time T .

3.1 Simulation 1

The position of the particles at $t = 3000$ is reported in Fig. 4. The rain starts with the particles at rest. We suppose that the speed of the landslide is much bigger than the rain flux, so that the computation of sliding is performed without the contribution of rain (i.e., instantaneously). The rain increases the mass of the particle with a factor between 0 and 0.0001. The graph of the kinetic energy (Fig. 5) shows a "stick-slip" dynamic. The distribution $f(x)$ the kinetic energy (Fig. 6) is well approximated by an exponential

$$f(x) = a \cdot e^{bx}, \tag{19}$$

with $a \simeq 3.2 \cdot 10^4$ and $b \simeq -0.1042$.

In Fig. 7 the statistical distribution of the intervals between trigger times is reported. This distribution is well fitted by a power law

$$f(x) = a \cdot x^b, \tag{20}$$

with $a \simeq 691.1$ and $b \simeq -0.4295$.

Several authors have observed that some natural hazards such as landslides, earthquakes and forest fires exhibit a power law distribution [10–12].

3.2 Simulation 1b

In this simulation we use the same parameters as in simulation 1, but we stop the rain event at time $t = 20$. This is a special case: we want to study the effect of a steady rain until a fixed time. Fig. 8 shows the arrangement of the particles and Fig. 9 the kinetic energy at $t = 300$.

One can note that the maximum kinetic energy is much greater in this simulation. In the case 1 the maximum value of kinetic energy is $5.74 \cdot 10^{-4}$ while here it is $2.6 \cdot 10^{-3}$. Many small events are observed in the first case while in the present one we observe a single large event.

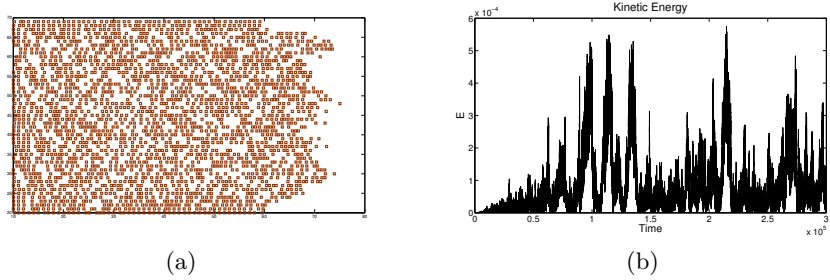


Fig. 4. (a) Position of particles in Simulation 1 at $t = 3000$.

Fig. 5. (b) Kinetic energy vs. time.

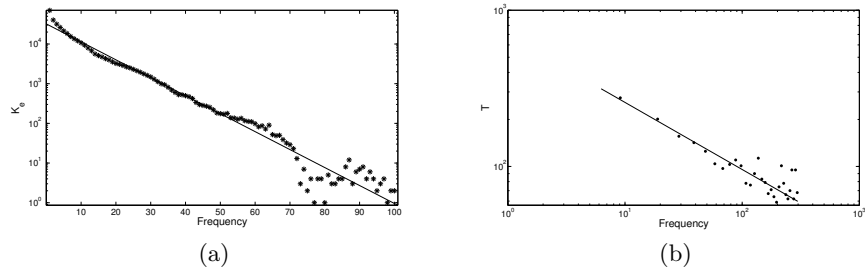


Fig. 6. (a) Frequency distribution of the kinetic energy in Simulation 1. The plot in semi-log axes shows an exponential distribution.

Fig. 7. (b) Frequency distribution of trigger intervals in Simulation 1. The plot in log-log axes shows a power-law distribution.

3.3 Simulation 2

In order to explore the dependence of the system behavior on the coefficient of cohesion c' , we vary it from 0.01 to 1. The other parameters are the same of Simulation 1. We observe that the final disposition of the particles (Fig. 10) is not too different from Simulation 1 (Fig. 4), however, it occurs at time $t = 7500$ versus $t = 3000$ of Simulation 1.

As reported in Fig. 11, the increase of the cohesion coefficient c' causes a time dilatation, i.e., a translation of the time at which similar events occur.

3.4 Simulation 3

We explore here the behavior of the system as a function of coefficients of static and dynamic friction μ_s and μ_d . Their values are shown in Table 1. The other parameters are the same of Simulation 1. The consequence of the reduction of friction causes an immediate movement of particles. Moreover the number of particles involved during the event are larger then in the previous simulations (Fig. 13).

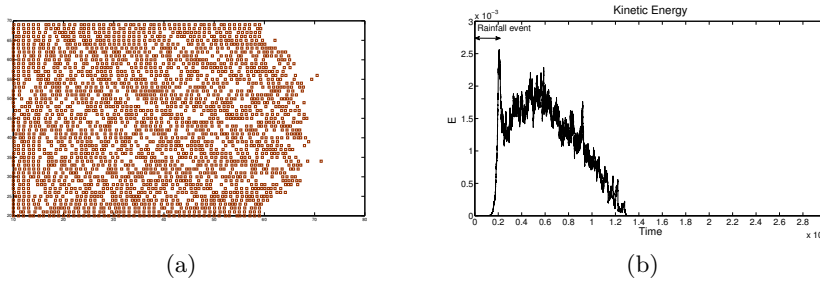


Fig. 8. (a) Position of particles in Simulation 1b at $t = 300$.

Fig. 9. (a) Kinetic energy versus time. We observe that the "stick-slip" events disappear and the fixed duration of precipitation changes the dynamics of the system: in particular, there is peak at $t = 20$ at the end of the rain event.

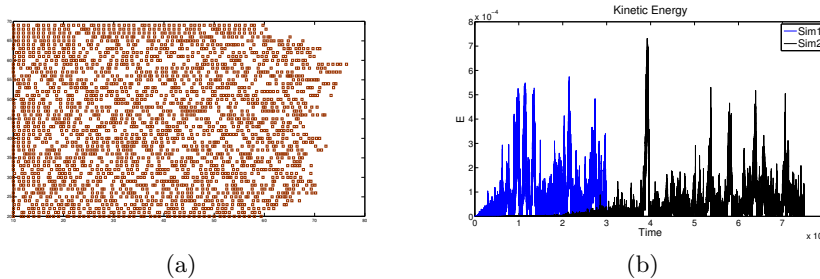


Fig. 10. (a) Position of particles in Simulation 2 at $t = 7000$. We observe that to have a spatial arrangement of particles similar to those of the previous simulation (Fig. 4) a larger time is needed.

Fig. 11. (b) Kinetic energy of the systems versus time. The black line is the kinetic energy of Simulation 2. Comparing it with Fig. 5 of Simulation 1, we observe that an increase in the cohesion coefficient induces a translation of the events.

Fig. 16 shows that also in this case the statistical distribution of the kinetic energy follows an exponential distribution. The data fit of Eq. (19) gives $a \simeq 2.592 \cdot 10^4$ and $b \simeq -0.091$.

4 Conclusions

In this article we presented a theoretical model that may be useful for studying the effect of precipitation on granular materials. The main hypothesis is that the rain acts as a lubricant between the terrain and the granular: this effect has been modeled by a preliminary report that includes the reduction of static (or dynamic) friction when we simulate the rainfall (Eq. (8) and Eq. (11)). The reduction in friction allows to follow the evolution and change in the position of the particles during and after a rainfall. The results obtained are very encouraging as regards both the displacement and evolution of the particles and

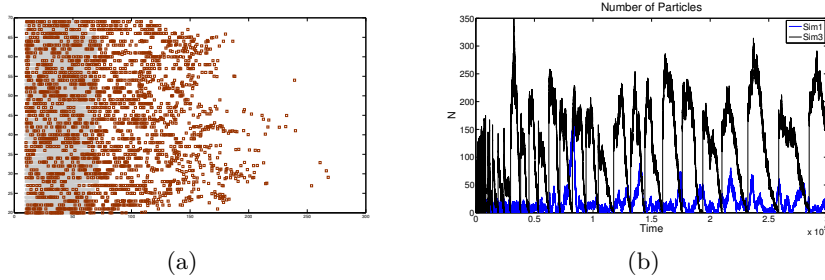


Fig. 12. (a) Position of particles in Simulation 3 at $t = 3000$. The gray area represents the particle position of Simulation 1 (Fig. 4).

Fig. 13. (b) Number of particles involved. The decrease of the friction coefficients leads to an increase in the number of particles in motion.

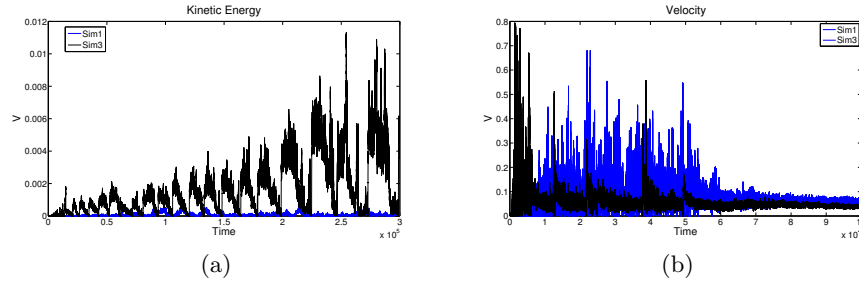


Fig. 14. (a) Kinetic energy of the systems vs. time. The black line is the kinetic energy of Simulation 3. In the last simulation the value of the kinetic energy is greater than that in Simulation 1. This is due to the number of particles involved in the event (Fig. 13).

Fig. 15. (b) Mean velocity of the system versus time after $t = 1000$ for Simulations 1 and 3. We can observe that the two values are not too different between the two simulations. The difference of the kinetic energy is due to the number of particle in movement.

in the statistical properties of the system. The next step will be to develop an experimental setup where granular material (sand or gravel) will be placed on a sloping surface: through liquid lubricant (soap and water) we will study the dynamics of these particles. The comparison of experimental and computational model will be very useful for the analysis of the effect of lubrication of the soil caused by rainfall.

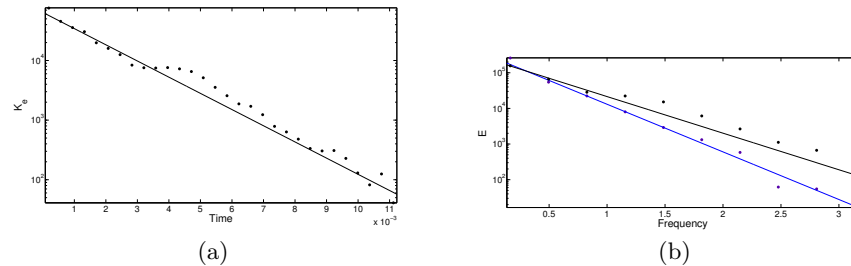


Fig. 16. (a) Statistical distribution of kinetic energy in Simulation 3. It follows an exponential distribution like in Simulation 1.

Fig. 17. (b) The blue line refers to Simulation 3 with parameters $a_3 \simeq 2.88 \cdot 10^5$ and $b_3 \simeq -2.365$. The black line refers to Simulation 1 with parameters $a_1 \simeq 2.83 \cdot 10^5$ and $b_1 \simeq -3.078$. The dots represent the normalized value of the respective simulations.

References

- 1.D.J. Varnes. Landslide type and processes. In: *Eckel E.B., ed., Landslides and engineering practice. National Research Council Highway Research Board Spec. Rept., Washington, D.C., (29):20–47, 1958.*
- 2.D.M. Cruden. A simple definition of a landslide. *Bulletin of the International Association of Engineering Geology*, (43):27–29, 1991.
- 3.D.J. Varnes. Slope movement types and processes. In: *Schuster R.L., Krizel R.J., eds., Landslides analysis and control. Transp. Res. Board., Special report 176, Nat. Acad. Press., Washington, D.C., (29):11–33, 1978.*
- 4.G.B. Crosta and P. Frattini. Rainfall-induced landslides and debris flows. *Hydrol. Process.*, (22):473–477, 2007.
- 5.S. Segoni, L. Leoni, A.I. Benedetti, F. Catani, G. Righini, G. Falorni, S. Gabelani, R. Rudari, F. Silvestro, and N.Rebora. Towards a definition of a real-time forecasting network for rainfall induced shallow landslides. *Natural Hazards and Earth System Sciences*, (9):2119–2133, 2009.
- 6.G.B. Crosta, S. Imposimato, and D.G. Roddeman. Natural hazards and earth system sciences. *Nat. Hazards Earth Syst. Sci.*, (3):523–538, 2003.
- 7.A.K. Patraa, A.C. Bauera, C.C. Nichitab, E.B. Pitmanb, M.F. Sheridanc, M. Bursikc, B. Ruppcc, A. Webberc, A.J. Stintonc, L.M. Namikawad, and C.S. Renschlerd. Parallel adaptive numerical simulation of dry avalanches over natural terrain. *Journ. of Volc. and Geot. Res.*, (139):1–21, 2005.
- 8.Ivan Iordanoff, Daniel Iliescu, Jean Luc Charles, and Jerome Neauport. Discrete element method, a tool to investigate complex material behaviour in material forming. *AIP Conference Proceedings*, 1252(1):778–786, 2010. doi: 10.1063/1.3457634. URL <http://link.aip.org/link/?APC/1252/778/1>.
- 9.L. Verlet. *Physycal Review*, (159):98, 1967.
- 10.D.L. Turcotte and B.D. Malamud. Landslides, forest fires, and earthquakes:examples of self-organized critical behavior. *Physica A*, (340):580–589, 2004.
- 11.D.L. Turcotte. Fractals and chaos in geology and geophysics. *Cambridge University Press, Cambridge*, (2nd Edition), 1997.

12. B.D. Malamud, D.L. Turcotte, F. Guzzetti, and P. Reichenbach. Landslide inventories and their statistical properties. *Earth Surface Processes and Landforms*, (29):687–711, 2004.